Proceedings of the
44th IEEE Conference on Decision and Control, and
the European Control Conference 2005
Seville, Spain, December 12-15, 2005

TuA18.3

Model Predictive Control of a Parallel Hybrid Vehicle Drivetrain

R. Beck*, S. Saenger$^{\|}$, F. Richert*, A. Bollig*, K. Neiß$^{\|}$, T. Scholt$^{\|}$, K.-E. Noreikat$^{\|}$, D. Abel*

*Institute of Automatic Control, RWTH Aachen University, Aachen, Germany

$^{\|}$DaimlerChrysler AG, Stuttgart, Germany

Abstract— **Hybrid vehicles gain importance and attention as the need for more fuel-efficient propulsion concepts increases. This article describes the modelling and the control of the longitudinal dynamics of a hybrid vehicle with a parallel configuration. The key aspect of the displayed hybrid concept is the smooth but quick transition between pure electrical driving and hybrid driving which has to occur without interruption of the demanded driving power and jerk. A model predictive control concept is presented for solving this task.**

I. INTRODUCTION

The development of new automotive engine and powertrain concepts is driven by the aim to reduce the average fleet CO_2 emissions and the increase of fuel economy. Long term improvements are expected from fuel cell powered vehicles but it is assumed that this technology will not reach the start of production before 2020 [1]. Hybrid powertrain concepts, in addition to the conventional internal combustion engine (ICE), are equipped with one or more electrical machines and a battery as energy storage unit. By utilising the specific advantages of the two power sources, hybrid vehicles are considered a short term possibility to achieve the mentioned goals. By driving electrically at low power demands, the inefficient part load operation of the combustion engine can be avoided. The fuel economy potential is estimated with up to 18% [2]. Additionally, the hybrid specific advantages like recuperation of energy during breaking or the realisation of a start/stop-functionality can further reduce the fuel consumption by another 7% [2]. Especially within city driving patterns this yields to an important reduction of pollutants, since at low velocities pure electrical driving is possible. However, a hybrid vehicle should not only be regarded for its fuel saving potential but also for its additional driving comfort and add on performance. The aspect covered by this article is the transition between pure electrical and hybrid driving where the ICE operates together with the electrical machines. For comfort reasons, the coupling needs to be as smooth as possible, meaning that an intermission in wheel torque is as unacceptable as a noticeable jerk. Several control approaches for smooth clutch engagement without induced drivetrain oscillations for conventional powertrains equipped with automated manual transmissions have been presented, including backstepping control [3], optimal control [4] and model predictive control [5]. In this article, the model predictive approach is developed further and applied to a clutch engagement situation in a hybrid powertrain presenting the usage of the specific benefits of the hybrid drivetrain architecture leading to a further enhancement of comfort and jerk reduction.

II. SYSTEM ARCHITECTURE

Figure 1 displays the composition of the considered hybrid powertrain developed by DaimlerChrysler. The so called P12-configuration is a parallel setup consisting of one conventional ICE and two electrical machines MG1 and MG2. A clutch separates the drivetrain into two sections: ICE with MG1 from MG2 and the rest of the transmission. The rear wheel driven vehicle is equipped with a standard automated gearbox without torque converter. The first electric machine MG1 serves mainly as a starter and a generator. During pure electrical driving, the clutch is opened and a series hybrid configuration is achieved. In this operating range, the second electric machine MG2 propels the vehicle. By closing the clutch, the configuration is changed into parallel mode, whereas all three power suppliers are lumped together. The transition from series mode into parallel mode occurs at low speeds up to $50\,\text{km/h}$. The critical aspect of careful synchronising the two drivetrain parts combined with the fast closing of the clutch is the focus of the work presented here.
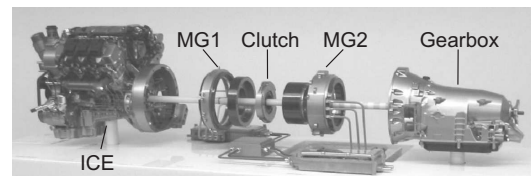

Fig. 1. P12-configuration of the hybrid powertrain [Source: Detroit Motor Show 2004]

III. SYSTEM MODELLING

Two models of different complexity were developed. Firstly, a multi-body model was built using the modelling tool DYMOLA. This model serves primarily as a testing environment for the designed control algorithm. Additionally, as a basis for the model predictive control algorithm, a second simplified model of the drivetrain was deduced from the complex one.

A. Complex DYMOLA Model

DYMOLA is based upon the modelling language "Modelica" and provides a graphical user interface to facilitate an easy setup of Modelica-models. The reasons for choosing DYMOLA to build the detailed powertrain model

are the advantageous object-oriented modelling language and the sophisticated numerical capabilities in handling mixed discrete-continuous models especially for realtime applications. A detailed description of the model is omitted here, since it is not within the scope of this paper to depict the usage of DYMOLA and the modelling of the drivetrain components. The model was verified against data obtained from drive tests conducted with the prototype hybrid vehicle where it performed well.

B. Simplified Model

A simplified mechanical model for the hybrid drivetrain was derived from the configuration displayed in Fig. 2. The first part of the powertrain can be approximated by
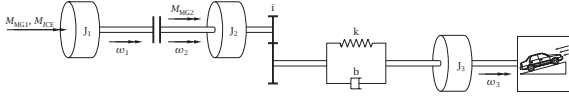

Fig. 2.   Simplified drivetrain structure

a lumped inertia J_1. Thereby the shaft holding ICE, MG1 and one clutch plate is modelled as a rigid body which is a valid approximation due to its high stiffness and the small inertias of the rotating parts. As proposed in [3] and [6] the second part of the powertrain is modelled by two inertias J_2 and J_3 connected by a spring with spring constant k and a damper with damping coefficient b and a resistance model combining all losses within the drivetrain and the driving resistances. The gearbox and the differential are modelled as a simple gain transforming the torques and the rotational speeds by a variable factor i depending on the selected gear. Three separate parts contribute to the resistance model - the air drag, the rolling resistance and the combined mechanical losses in the gearbox, the differential and the shaft bearings due to friction. The latter part was approximated from measured characteristic curves as second order polynomials. Thus the resulting resistance torque M_v can be formulated as

$$M_v = \left(\frac{\rho}{2}c_w A(r\omega_3)^2 + f_r mg\right) r + a_0 + a_1\omega_3 + a_2\omega_3^2 \quad (1)$$

with the air density ρ, the drag coefficient c_w the vehicle's frontal area A, the wheel dynamic radius r, the resistance coefficient f_r, the vehicle's mass m and the identified polynomial coefficients a_i. The influence of road inclination leading to an additional accelerating or decelerating torque and an altered rolling resistance due to a change in normal force is not considered and can be seen as a disturbance to the system similar to a changing vehicle's mass. Since the developed powertrain model is used for low vehicle speeds, where the contribution of the terms proportional to ω_3^2 to M_v is small, the linearisation

$$M_v = M_{v0} + k_v\omega_3 \quad (2)$$

is possible without significant loss of accuracy. Due to the different gear ratios, the coefficients M_{v0} and k_v vary for each gear.

Two different modes of the drivetrain must be distinguished - the closed clutch situation where the clutch behaves as a rigid bond and the mode with opened or sliding clutch. At first the open/sliding clutch mode shall be considered. For the first part of the powertrain the equation

$$M_{1o} = J_1\dot{\omega}_1 \quad (3)$$

can be derived. The driving torque M_{1o} is calculated by

$$M_{1o}(s) = M_{ICE} + M_{MG1} - M_c \quad (4)$$

with the torques M_{ICE} and M_{MG1} of the combustion engine and the electric machine and the friction torque M_c transmitted by the clutch which is computed by

$$M_c = \mu r F_{nc}\text{sign}(\omega_1 - \omega_2) \quad (5)$$

where μ denominates the clutch friction coefficient, r the effective clutch radius and F_{nc} the normal force exerted on the clutch. For the second drivetrain part the following two equations

$$M_{2o} = J_2\dot{\omega}_2 i + J_3\dot{\omega}_3 + k_v\omega_3 \quad (6)$$

and

$$\dot{M}_{2o} = J_2\ddot{\omega}_2 i + b\left(\frac{\dot{\omega}_2}{i} - \dot{\omega}_3\right) + k\left(\frac{\omega_2}{i} - \omega_3\right) \quad (7)$$

are obtained. The torque M_{2o} is given by

$$M_{2o} = i\eta(M_{MG2} + M_c) - M_{v0} \quad (8)$$

with the combined efficiency η of the gearbox and the differential. Combining (3)-(8) and approximating the actuator dynamics of the electric machines and the combustion engines by first order lag systems with a time constant of $\tau = 0.1\,\text{sec}$ the state space model

$$\dot{\mathbf{x}}_o = \begin{pmatrix} 0 & 0 & 0 & 0 & \frac{1}{J_1} & \frac{1}{J_1} & 0 \\ 0 & 0 & -\frac{k_v}{J_2 i} & -\frac{J_3}{J_2 i} & 0 & 0 & \frac{\eta}{J_2} \\ 0 & 0 & 0 & 1 & 0 & 0 & 0 \\ 0 & \frac{k}{J_3 i} & -\frac{kJ_2 i^2 + bk_v}{J_2 J_3 i^2} & -\frac{k_v + b}{J_3} - \frac{b}{J_2 i^2} & 0 & 0 & \frac{b\eta}{J_2 J_3 i} \\ 0 & 0 & 0 & 0 & \frac{-1}{\tau} & 0 & 0 \\ 0 & 0 & 0 & 0 & 0 & \frac{-1}{\tau} & 0 \\ 0 & 0 & 0 & 0 & 0 & 0 & \frac{-1}{\tau} \end{pmatrix}\mathbf{x}_o$$

$$+ \begin{pmatrix} 0 & 0 & 0 & \frac{-1}{J_1} & 0 \\ 0 & 0 & 0 & \frac{\eta}{J_2} & \frac{-1}{J_2 i} \\ 0 & 0 & 0 & 0 & 0 \\ 0 & 0 & 0 & \frac{b\eta}{J_2 J_3 i} & \frac{-b}{J_2 J_3 i^2} \\ \frac{1}{\tau} & 0 & 0 & 0 & 0 \\ 0 & \frac{1}{\tau} & 0 & 0 & 0 \\ 0 & 0 & \frac{1}{\tau} & 0 & 0 \end{pmatrix}\mathbf{u}_o \quad (9)$$

with $\mathbf{u}_o = \begin{pmatrix} M_{ICE}^{in} & M_{MG1}^{in} & M_{MG2}^{in} & M_c & M_{v0} \end{pmatrix}^T$ and $\mathbf{x}_o = \begin{pmatrix} \omega_1 & \omega_2 & \omega_3 & \dot{\omega}_3 & M_{ICE} & M_{MG1} & M_{MG2} \end{pmatrix}^T$ is obtained.

Since the choice of J_2, J_3, k and b is not intuitive the four parameters were determined for each gear by parametric identification applying random step inputs to the complex

DYMOLA model and matching the measured rotational speeds ω_2 and ω_3.

For the closed clutch mode the system's degree of freedom is reduced since obviously

$$\omega_1 = \omega_2 \tag{10}$$

holds. Equations (6) - (8) change slightly yielding

$$\dot{\mathbf{x}}_c = \begin{pmatrix} 0 & -\frac{k_v}{J_{2c}i} & -\frac{J_3}{J_{2c}i} & \frac{\eta}{J_{2c}} & \frac{\eta}{J_{2c}} & \frac{\eta}{J_{2c}} \\ 0 & 0 & 1 & 0 & 0 & 0 \\ \frac{k}{J_3 i} & -\frac{kJ_{2c}i^2+bk_v}{J_{2c}J_3 i^2} & -\frac{k_v+b}{J_3}-\frac{b}{J_{2c}i^2} & \frac{b\eta}{J_{2c}J_3 i} & \frac{b\eta}{J_{2c}J_3 i} & \frac{b\eta}{J_{2c}J_3 i} \\ 0 & 0 & 0 & \frac{-1}{\tau} & 0 & 0 \\ 0 & 0 & 0 & 0 & \frac{-1}{\tau} & 0 \\ 0 & 0 & 0 & 0 & 0 & \frac{-1}{\tau} \end{pmatrix} \mathbf{x}_c$$

$$+ \begin{pmatrix} 0 & 0 & 0 & \frac{-1}{J_{2c}i} \\ 0 & 0 & 0 & 0 \\ 0 & 0 & 0 & \frac{-b}{J_{2c}J_3 i^2} \\ \frac{1}{\tau} & 0 & 0 & 0 \\ 0 & \frac{1}{\tau} & 0 & 0 \\ 0 & 0 & \frac{1}{\tau} & 0 \end{pmatrix} \mathbf{u}_c \tag{11}$$

with $\mathbf{x}_c = (\omega_2 \quad \omega_3 \quad \dot{\omega}_3 \quad M_{ICE} \quad M_{MG1} \quad M_{MG2})^T$, $\mathbf{u}_c = (M_{ICE}^{in} \quad M_{MG1}^{in} \quad M_{MG2}^{in} \quad M_{v0})^T$, $J_{2c} = J_1 + J_2$.

The simplified model was also validated at low speeds against drive test data where it performed well (Fig. 3). The
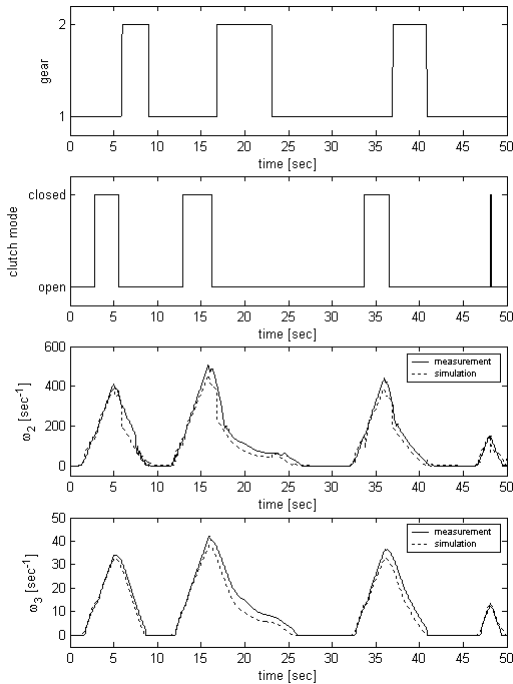

Fig. 3. Validation of the simplified model

described simplified model is nonlinear due to the different gears, the two clutch modes and the changing sign in (5) but it consists of linear subsets which significantly reduces the computational cost during simulation and eases the model predictive control described in the following section.

IV. TRANSITION CONTROL

A. Control structure

The task of the controller is to accomplish the transition between electrical and hybrid driving. A superordinate control requires this transition depending on the vehicle's speed and the power demand of the driver. Before the developed controller starts its action the ICE is started with the help of MG1 and is running at idle speed. There are four control inputs available - the torques M_{ICE}, M_{MG1} and M_{MG2} of the engine and the electric machines and the normal force F_{nc} applied to the clutch. Analysing the drivetrain (Fig. 2) it is obvious, that only two of these controls can be used as independent optimisation variables within the MPC since M_{ICE}, M_{MG1} and M_c act upon the same shaft as well as M_{MG2} and M_c. Therefore the trajectory of F_{nc} during the clutch engagement is chosen as a design parameter. Depending on the actual clutch setup this trajectory is determined externally by the clutch controller after the onset of the engagement process or can be chosen by the MPC. In either case the future trajectory of F_{nc} is known and can be exploited for the predictive control. The current drivetrain contains a dry clutch where F_{nc} is increased linearly from 0 to its maximum value by the clutch controller after receiving the request to close the clutch. With F_{nc} as a design parameter $M_{ICE}+M_{MG1}$ and M_{MG2} are selected as outputs of the MPC. How to split $M_{ICE} + M_{MG1}$ is a question of the individual constraints and fuel efficiency. This task is carried out by a simple splitting strategy.

The measurements available are the rotational speeds ω_1, ω_2 and ω_3. These are used to realign the controller's internal model using a Kalman filter as state observer.

The two main goals that have to be accomplished by the transition controller are the fast synchronisation of the two drivetrain parts and the realisation of the transition without interrupting the driving power and without sensible jerk. It is obvious, that these two objectives are directly opposed since a fast synchronisation could be achieved by rapidly slowing down ω_2 which would lead to an unacceptable jerk. Therefore it was decided to implement a two-stage MPC with two separate cost functions instead of just one MPC with one combined cost function leading to a trade-off optimal solution. This control structure is displayed in Fig. 4.

The first MPC accomplishes the task of a comfortable transition and the avoidance of driving power interruption. This is done by minimising the cost function

$$J_{c,1} = \sum_{k=N_1}^{N_2} \frac{1}{2} \left(M_d - i\eta (M_{MG2} + M_c) \right)^2 \quad . \tag{12}$$

The interval $[N_1, N_2]$ denominates the prediction horizon of the controller. The future trajectory of the driver's torque demand at the wheels M_d is not known but assumed to remain constant at the current value determined from the
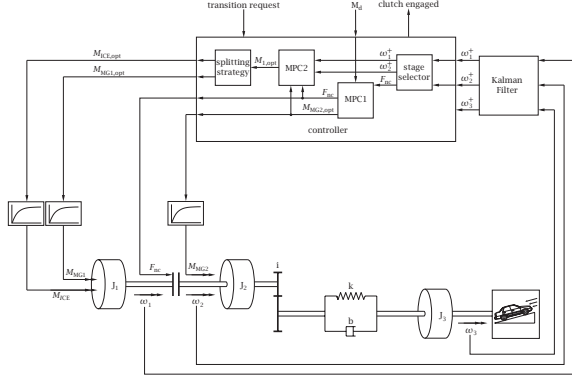
Fig. 4.   Control structure

accelerator. This assumption is valid because on the one hand the time constant of human reaction of 0.1 sec is one order of magnitude greater than the sampling rate of the controller and on the other hand the accelerator signal is normally filtered quite heavily. Therefore only moderate changes of M_d are expected within the control horizon. The choice of the cost function $J_{c,1}$ is based on the following considerations. First of all the transition must be carried out without interruption of driving power. This is accomplished if the torque $i\eta(M_{MG2} + M_c)$ follows the driver's demand. Secondly, neglecting the velocity-dependent resistance terms and the drivetrain elasticity, the jerk $\ddot{\omega}_3$ is direct proportional to the time derivative of the driving torque at the wheels $\frac{d}{dt}i\eta(M_{MG2} + M_c)$. Therefore for a constant driver's demand M_d the minimisation of $J_{c,1}$ will also minimise the jerk $\ddot{\omega}_3$. Any jerk induced by a variation of M_d is desired by the driver and must therefore not be suppressed.

The second MPC addresses the goal of synchronising the two drivetrain parts. With the known trajectory M_c and the optimised trajectory $M_{MG2,opt}$, which is the output of the first MPC, the future trajectory $\hat{\omega}_2$ can be predicted by the controller's internal model. Minimising the cost function

$$J_{c,2} = \sum_{k=N_1}^{N_2} \frac{1}{2}(\hat{\omega}_2 - \omega_1)^2 \quad . \tag{13}$$

leads to an optimal control sequence $M_{ICE} + M_{MG1}$ which equals the rotational speeds of the drivetrain parts.

The transition is accomplished in three stages. During the first stage the clutch is not actuated. This is mainly due to excessive wear of the clutch material at high slip velocities. When the difference of the rotational velocities ω_1 and ω_2 reaches a specified target corridor the second stage is initiated during which the clutch engagement is started. After the clutch is closed, the additional inertia J_1 is compensated in order to avoid jerk. The following paragraphs focus on special aspects of the three stages.

B. Stage 1: Synchronisation of drivetrain parts

Since the clutch torque M_c is 0 during this stage, the torque delivered by MG2 is only determined by the driver's demand as in the pure electrical driving mode. The main task during this stage is to diminish the speed difference between the drivetrain parts as quick as possible. For this purpose a larger control horizon N_u is chosen. $N_u = 1 \ldots 3$, $N_1 = 1$ and $N_2 = 10 \ldots 20$ lead good results. It is preferred to start the clutch engagement from a situation $\omega_1 > \omega_2$. In this case M_c is positive (5) and thereby assists MG2 in satisfying the driver's torque demand. If $\omega_1 < \omega_2$ MG2 would have to supply additional torque in order to compensate the negative effect of M_c. In many cases this might not be possible for MG2 is already operating near its maximum power when the transition is requested. In order to reach a situation where $\omega_1 > \omega_2$ before advancing to stage 2, (13) is modified slightly to

$$J'_{c,2} = \sum_{k=N_1}^{N_2} \frac{1}{2}(\hat{\omega}_2 + \Delta\omega_{p1} - \omega_1)^2 \tag{14}$$

with $\Delta\omega_{p1} > 0$. Since gear changes are inhibited by the superordinate control during the transition process, the drivetrain model is linear and minimising $J'_{c,2}$ leads to a constrained quadratic optimisation problem which reduces the computational cost significantly ([7], [8]).

C. Stage 2: Clutch engagement

After $\omega_1 - \omega_2$ reaches a target corridor the clutch engagement is requested. From the clutch characteristics the future trajectory M_c can be calculated and the effect of the clutch torque is compensated by minimising $J_{c,1}$ in order to impede jerk caused by the clutch engagement. The minimisation of $J_{c,2}$ is carried out with a smaller control horizon of $N_u = 1$ and a larger prediction horizon in order to reduce the remaining speed difference smoothly. The end of the engagement process is detected when the measured speed difference falls below a specified limit and a minimum normal force is exerted which allows the transmission of the applied torques. This minimum normal force can be approximated from simple mechanical considerations to

$$F_{nc,min} \approx$$
$$\frac{\left| J_{23}(M_{MG1} + M_{ICE}) - J_1\left(\eta M_{MG2} - \frac{M_v}{i}\right) \right|}{\left(J_1\eta + J_2 + \frac{J_3}{i^2}\right)\mu r} \tag{15}$$

with $J_{23} = J_2 + \frac{J_3}{i^2}$. Assuming that the sign in (5) does not change during this stage, the linearity of the drivetrain model is conserved. This assumption is valid, since, due to the small control horizon and the larger prediction horizon combined with the rapid increase of the normal force, the difference $\omega_1 - \omega_2$ converges to 0 asymptotically.

D. Stage 3: Compensation of additional inertia

After stage 2 of the synchronisation is completed the transition is concluded. The superordinate control resumes the drivetrain regulation. One important aspect of the clutch mode change from sliding to stuck mode at time t^* is the sudden addition of inertia which leads to a discontinuity in the resulting acceleration $\dot{\omega}_2$ in case of a constant net torque at the gearbox input which is determined from

$$M_{n,o} = M_{MG2} + M_c \tag{16}$$

for the sliding clutch and

$$M_{n,c} = M_{ICE} + M_{MG1} + M_{MG2} \tag{17}$$

for the closed clutch ([4]). In order to compensate this effect the net torque is increased yielding

$$M_{n,c}(t^{*+}) = M_{n,o}(t^{*-}) \frac{(J_1 + J_2)i^2 + J_3}{J_2 i^2 + J_3} \quad . \tag{18}$$

V. RESULTS

For studying the potential of the developed control algorithm simulations were carried out using the complex DYMOLA model as the system's representation. Since important parameters of the vehicle dynamics can change, much attention has been paid to the robustness of the controller. The internal model of the controller is parametrised according to a vehicle mass of $m = 2000\,\mathrm{kg}$. As mentioned above, the road inclination s is not accounted for by the simplified model. These two parameters are identified to have the largest impact on the drivetrain dynamics. Additionally the effect of changes in the clutch friction coefficient due to wear has been investigated.

In all simulations the controller worked with a sampling time of $T = 0.01\,\mathrm{sec}$.

A. Nominal conditions

The following simulations were conducted with the DYMOLA model using the nominal parameters $m = 2000\,\mathrm{kg}$, $s = 0$ and $\mu = 0.26$. Figure 5 shows a transition at low speeds around $16\frac{\mathrm{km}}{\mathrm{h}}$ in first gear. The vehicle is launched at $0.5\,\mathrm{sec}$ by MG2. The torque delivered by MG2 is increased up to $200\,\mathrm{Nm}$. At $2.5\,\mathrm{sec}$ the engine is started and at $3.0\,\mathrm{sec}$ the developed controller is requested to engage the clutch. The synchronization happens fast and nearly without jerk. At approximately $3.4\,\mathrm{sec}$ the clutch is fully engaged. Comparing the induced jerk due to the clutch engagement with the jerk during the start of the vehicle one can conclude that it is small.

Figure 6 displays the results of a transition at a high vehicle speed around $45\frac{\mathrm{km}}{\mathrm{h}}$ in second gear. The controller performance does not suffer from the higher speed and it can be concluded that the negative effect of the linearisation of (1) is small.

The simulations presented in Fig. 5 and 6 were carried out using a constant driver's torque demand throughout the
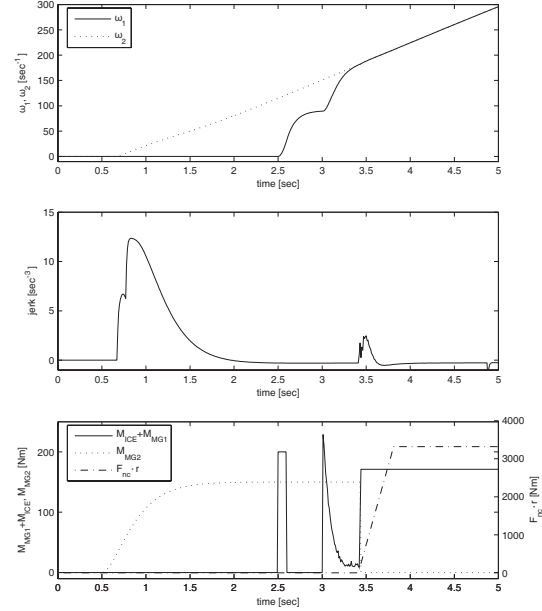

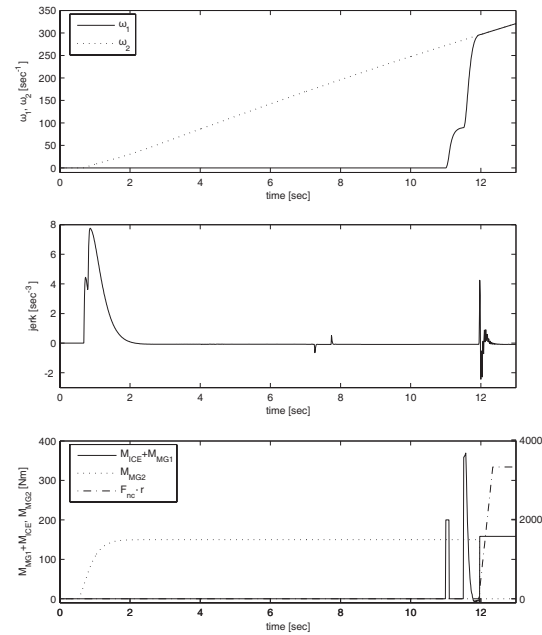Fig. 5.   Transition at nominal conditions at low speed

Fig. 6.   Transition at nominal conditions at high speed

transition which corresponds exactly to assumption made for setting up the cost function $J_{c,1}$. Figure 7 shows the result of a transition conducted with severe variations of the driver's torque demand. It can be seen, that the controller performs well and again it is pointed out, that the jerk due to changes of the driver's torque request is much higher than the jerk induced during the transition.

B. Robustness

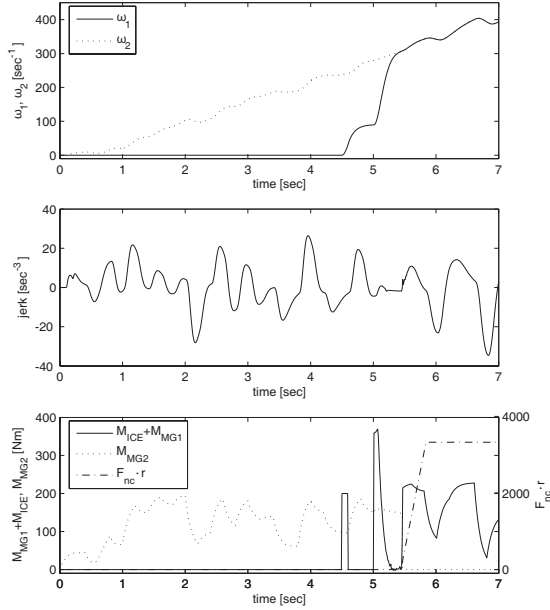Since the controller has to be reliable under varying driving conditions, the robustness of the control algorithm

2674

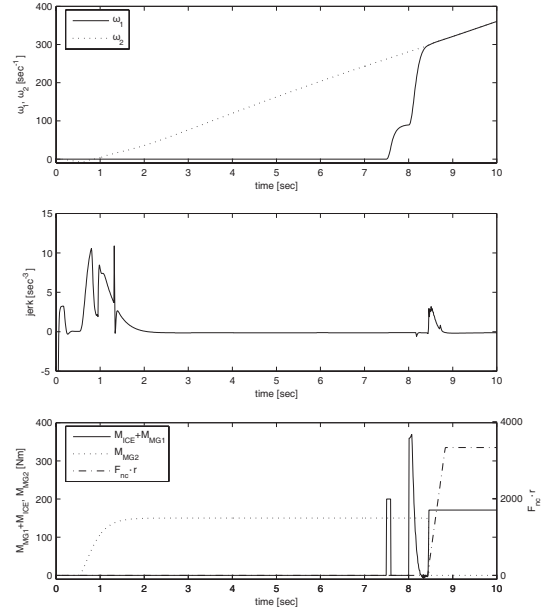Fig. 7.   Transition at nominal conditions with varying M_d

Fig. 9.   Transition with $m = 2500 \, \text{kg}$, $s = +5\%$ and $\mu = 0.195$

regarding changes in the vehicle's behaviour is an important issue. Figures 8 and 9 display the results obtained. Figure 8 shows a synchronisation at around $40 \frac{\text{km}}{\text{h}}$ with a low vehicle mass of $m = 1700 \, \text{kg}$, a road inclination of $s = -5\%$ and a friction coefficient of $\mu = 0.195$ (-25%). The transition presented in Fig. 9 was conducted with $m = 2500 \, \text{kg}$, $s = +5\%$ and $\mu = 0.195$. The controller performance does not suffer from these severe parameter changes and it can be concluded that the controller is robust regarding changes of the vehicle dynamics.
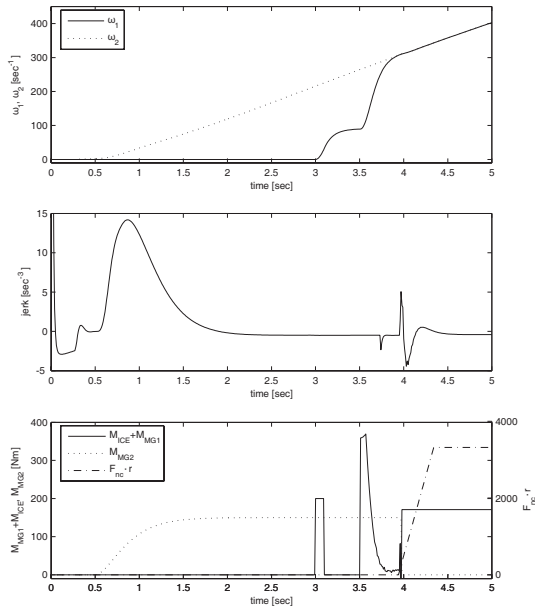

Fig. 8.   Transition with $m = 1700 \, \text{kg}$, $s = -5\%$ and $\mu = 0.195$

VI. CONCLUSIONS AND FUTURE WORK

A model predictive control for a hybrid drivetrain was presented. The conducted simulations exhibit a good and robust performance of the controller. Further work will focus on the application to the real drivetrain. The algorithm will be implemented into an electronic control unit and applied to a test drivetrain. Additionally the effect of variable uncertain time delays due to the vehicle's internal non-deterministic CAN-communication will be examined. The performance of the controller will be examined in drive tests and compared to alternative control algorithms.

REFERENCES

[1] J.-W. Biermann, C. Bunz, M. Crampen, S. Köhle, and D. Mesiti, "Three OEM, One Common Powertrain Concept - Three New Hybrid Cars, Developed in the EU-Project SUVA," in *Proc. of the Aachen Colloquium on Automobile and Engine Technology*, oct 2004, pp. 1203–1215.

[2] H. Kemper, M. Jentges, and O. Rütten, "Hybridization as Launch and Acceleration Improvement Technology," in *Proc. of the Aachen Colloquium on Automobile and Engine Technology*, oct 2004, pp. 923–934.

[3] J. Fredriksson and B. Egbert, "Nonlinear Control applied to Gearshifting in Automated Manual Transmissions," in *Proc. of the 39th IEEE Conference on Decision and Control*, dec 2000, pp. 444–449.

[4] F. Garofalo, L. Glielmo, L. Iannelli, and F. Vasca, "Optimal tracking for automotive dry clutch engagement," in *Proc. of the 15th IFAC world congress*, jul 2002.

[5] A. Bemporad, F. Borelli, L. Glielmo, and F. Vasca, "Hybrid control of dry cluth engagement," in *Proc. of the European Control Conference 2001*, sep 2001, pp. 635–639.

[6] B. K. Powell, K. E. Bailey, and S. R. Cikanek, "Dynamic Modelling and Control of Hybrid Electric Vehicle Powertrain Systems," *IEEE Control Syst. Mag.*, vol. 18, oct.

[7] P. Krauss, "Prädiktive Regelung mit linearen Prozessmodellen im Zustandsraum," Ph.D. dissertation, RWTH Aachen University, 1996.

[8] J. M. Maciejowski, *Predictive Control with Constraints*.   Pearson Education, 2002.